Pressure-Sensor-Based Sleep Status and Quality Evaluation System

Lih-Jen Kau, *Senior Member, IEEE*, Mao-Yin Wang, and Houcheng Zhou

***Abstract*—Sleep quality evaluation is a major approach to clinical diagnosis of different types of sleep and mental disturbances. How to render it possible for test subjects to complete sleep status detection and quality assessment in a natural environment is what this article mainly highlights. Clinically, sleep disturbances are analyzed by the so-called polysomnography (PSG). However, due to limitations in space and high cost, as well as the fact that test subjects must wear various types of physiological detection equipment during the test, the collected signal is susceptible to interference due to uncomfortable sensations. As such, it usually does not reflect the realistic situation of the subject. For this reason, we propose in this article a pressure-sensor-based smart mattress to realize sleep status detection and quality evaluation. Regarding sleep posture recognition, a proposed convolutional neural network (CNN) model in conjunction with a pressure distribution image formed by the pressure-sensing matrix is applied. With respect to assessing the subjects' time in bed, a support vector machine (SVM) is used to determine sitting or lying postures and further recognize the actual time in bed. As for sleep quality assessment, Fuzzy inference is adopted in this article based on a set of four predefined sleep parameters. Compared with some of prior arts, the proposed system does not require the test subjects to wear any equipment, and as such, the subjects can complete the test in a natural environment. Experimental results show that the accuracy of the proposed SVM classifier for differentiating sitting and lying posture and that of the CNN model for the recognition of four different sleep postures can be up to 99.986% and 96.987%, respectively. With the proposed model, precise sleep parameters, including time in bed, the number of times of bed leaving, the number of times of body movements all night, standard deviation of time interval between body movements, and sleep posture, can be provided. Moreover, the system does not use devices such as microphones or surveillance cameras to collect the data of the test subjects; thus, there is no concern about infringing the privacy of the subjects. It is believed that the system will be of considerable help and serve as an aid to clinical diagnosis of sleep disturbance.**

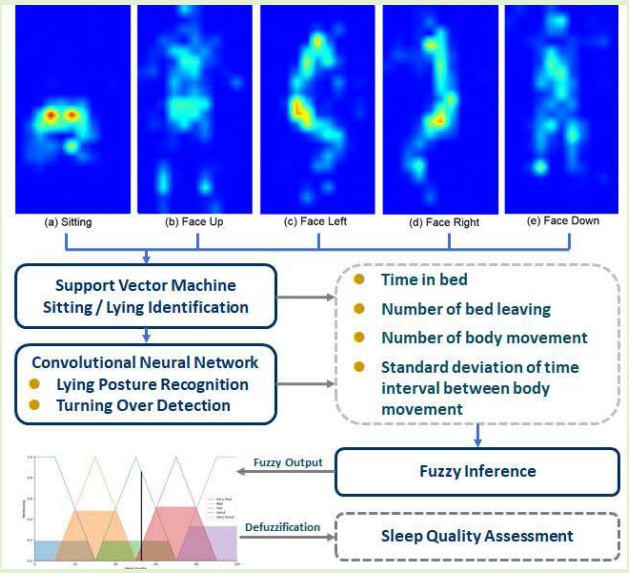

***Index Terms*— Fuzzy inference, machine learning, posture recognition, pressure sensing, sleep quality assessment.**

Manuscript received 3 March 2023; accepted 15 March 2023. Date of publication 3 April 2023; date of current version 1 May 2023. This work was supported in part by the National Science and Technology Council, Taiwan, under Grant MOST 109-2221-E-027-086-MY2. The associate editor coordinating the review of this article and approving it for publication was Prof. Kea-Tiong (Samuel) Tang. *(Corresponding author: Lih-Jen Kau.)*

This work involved human subjects or animals in its research. The authors confirm that all human/animal subject research procedures and protocols are exempt from review board approval.

Lih-Jen Kau is with the Department of Electronic Engineering, National Taipei University of Technology, Taipei 10608, Taiwan (e-mail: ljkau@mail.ntut.edu.tw).

Mao-Yin Wang is with the Department of Electronic Engineering, National Taipei University of Technology, Taipei 10608, Taiwan, and also with Silicon Application Corporation, Taipei 11568, Taiwan (e-mail: t102419006@ntut.edu.tw).

Houcheng Zhou was with the Department of Electronic Engineering, National Taipei University of Technology, Taipei 10608, Taiwan. He is now with the Shenzhen Health Development Research and Data Management Center, Shenzhen, Guangdong 518028, China (e-mail: joneschau@outlook.com).

Digital Object Identifier 10.1109/JSEN.2023.3262747

I. Introduction

GOOD sleep quality helps keep your mind and body healthy, repairing damaged cells, as well as regulating the circadian cycle of endocrine system [1], [2], [3]. According to the 2018 Sleep Quality Report and the data released by the World Association of Sleep Medicine (WASM) on the World Sleep Day (WSD) in 2019, the adult insomnia rate in China reached up to 38.2%, which was the equivalent of more than 300 million people in China suffering from sleep disturbance [3]. In addition, many research reports show that the cause of Alzheimer's disease is directly related to the presence of insomnia [4]. The research report from the not-for-profit research institute RAND Europe indicates the economic loss caused by sleep insufficiency in USA has reached U.S. $411 billion a year; more than one-third of adults have experienced sleep deprivation in USA [5]. For this reason, the U.S. Centers for Disease Control and Prevention (CDC) describes

sleep deprivation as a public health epidemic. The statistic from the National Highway Traffic Safety Administration (NHTSA) showed that there were more than 72 000 serious car crashes related to drowsy driving in 2015, which caused 41 000 injuries and more than 800 deaths [6]. Following the U.S. $411 billion economic loss in USA, Japan's U.S. $138 billion was the second largest economic loss indirectly due to sleep insufficiency, followed by Germany, U.K., and Canada [7]. According to survey data, approximately 1/10 of the population in Taiwan has been affected by insomnia [8]. Poor sleep quality can easily lead to metabolic inhomogeneity, decrease in immunity, dysautonomia, memory getting worse, as well as being more likely to suffer from the Three Highs [9]. It is obvious that the various problems derived from poor sleep quality are considerably serious.

To assess the problems related to sleep disturbance, questionnaire evaluation and professional instruments are mostly used in clinical practice. With respect to questionnaire evaluation, standardized questionnaires are usually used for evaluation. Types of questionnaires include Berlin Questionnaire, Epworth Sleepiness Scale (ESS), and Pittsburgh Sleep Quality Index (PSQI). Professional instruments used to evaluate sleep quality can be roughly divided into two types: contact devices and noncontact devices. Among contact devices, wearable sensing devices are mostly used, such as electrode patches, pressure sensors, blood oxygen measurement finger cuffs, respiration sensors, and sphygmomanometers, and all sensing devices should be connected to the detection instrument to integrally collect the subjects' physiological data [10], [11], [12], [13], [14], [15], [16], [17], [18], [19], [20], [21], [22], [23], [24], [25], [26], [27], [28], [29], [30]. For noncontact devices, the instruments, such as cameras, microphones, as well as radio frequency transceiver in millimeter wave (mmWave) or ultrawideband (UWB), are often used to detect the behavior of the subjects [31], [32], [33], [34], [35], [36].

Polysomnography (PSG) is mostly used as the basis for evaluating sleep quality in clinical practice. Before performing the PSG test, the medical staff places electrode patches on the test subject's chin, head, canthus, heart, and legs, while the pressure-sensing device is worn on the abdomen and chest. In addition, the blood oxygen measurement device is required to be put on the end of the finger, the respiration sensor is placed under the nose and in front of the mouth, the sphygmomanometer is placed snugly around the upper arm, and all the sensing devices are connected to the detection instrument for an integral parameter collection [10]. Although the important parameters, such as electrocardiography (ECG), electromyography (EMG), electrooculography (EOG), blood pressure, respiratory effort, electroencephalography (EEG), air flow, blood oxygen saturation (SpO2), heart rate, and sleep posture, can be obtained simultaneously through PSG, such detection method is expensive, and test subjects must wear various physiological detection equipment during the test, which is prone to causing uncomfortable sensations [11], as well as rendering it difficult to offer the best sleep quality assessment process.

To solve the inconvenience of the foregoing PSG, many sleep quality assessment systems and algorithms have been proposed. Quite a few low-complexity and low-cost wearable devices have been used in sleep quality and sleep status detection due to the popularity of wearable devices in recent years [12], [13], [14], [15], [16], [17]. In [12], a wrist motion recorder based on a triaxial accelerometer and motion density analysis was proposed to evaluate the user's sleep efficiency, total sleep duration, when to fall asleep, and the number of times of waking up after falling asleep. Literature [13] analyzes the characteristics of photoplethysmography (PPG) signal and sets a threshold value to realize the function of detection and wake-up of sleep apnea characteristics. Literature [14] analyzes the middle- and low-frequency band energy of heart rate variability (HRV) through PPG signals and evaluates the timing of sleep and wakefulness. Literature [15] combines an inertial measurement unit (IMU) with PPG to collect sleep or wake characteristics and uses a linear classifier to classify the status of sleep and arousal. In [16], a slow wave sleep estimation approach for healthy subjects and obstructive sleep apnea (OSA) patients is proposed by calculating the R–R intervals in ECG signal for heart rate variations analysis. In [17], an Internet of Things (IoT)-based wireless PSG system is implemented for sleep monitoring, and a Java-based PSG recording program is designed to record acquired biosignals. In [18], an automatic sleep stage scoring approach is proposed based on single-channel EEG and deep learning model. Literature [19] proposes a transfer learning method, which could overcome the data mismatch problem; however, it is unable to achieve real-time computing. A smart phone is used as a computing platform in [20] and the single-channel EEG is used as the signal source, and then, the proposed time-distributed convolutional neural network (CNN) algorithm is used to achieve real-time inference for deep or light sleep. To accelerate long-term sleep monitoring performance, an ultralow-power dual-mode automatic sleep staging processor is proposed by using a neural network (NN)-based decision tree classifier in [21].

Pressure-sensitive cushions are often used for the user's sitting, sleeping posture detection, as well as sleep quality assessment [22], [23], [24], [25], [26], [27], [28], [29]. In [22], a two-layer pressure-sensitive pad formed in an array with 44 rows and 52 columns is used to recognize seven types of sitting postures, and a very good classification accuracy up to 97.07% can be obtained with a proposed five-layer neural network classifier. Considering the balance between classification accuracy and hardware resource consumption, the authors also investigated a sensor array with fewer nodes and an accuracy of 96.26% can be maintained when an 11×13 sensor array in conjunction with the proposed Random Forest algorithm is used [22]. Literature [23] proposes an approach regarding the recognition of sleep status on high-resolution pressure-sensor-based bed sheet. By detecting the variability of respiratory symptom frequency, respiratory rate, leg exercises, turning over, and other characteristics, the mentioned characteristics are fed into a support vector machine (SVM) and k-nearest neighbors (KNN)-based classifier to differentiate the three

sleep stages, which are awake, rapid eye movement (REM) and nonrapid eye movement (NREM); however, such classification accuracy still needs to be improved. Literature [24] focuses on the classification of sleep stages as well. A small number of pressure sensors are applied to detect the sleep posture of the subjects but still encounter the same problem of low accuracy [24].

Sleep posture is a critical factor for evaluating sleep quality and preventing pressure sores; pressure distribution sensing system is a common method for sleep posture recognition. Literature [25] proposes a method of sleep posture recognition based on a so-called body-Earth mover's distance (BEMD); BEMD has the 2-D image of pressure distribution weighted and combines the Earth mover's distance (EMD) with Euclidean distance for similarity measurement. The experimental results show that the accuracy of BEMD in posture detection can reach 91.2%. Literature [26], [27] proposes a pressure-sensor-based noninvasive sleep assessment device. Such a device uses 24 force-sensitive resistors placed on the thoracic area of the mattress in an array of 8×3 and uses a multiplexer (MUX) to obtain the readings of each pressure sensor, and parameters related to time in bed, respiratory frequency, number of times of body movements, number of sleep apnea, and so on through the pressure value read therefrom. Due to the small number of pressure sensors used, the test subject may sit on the pressure-sensing array instead of lying on it; thus, this structure has a misinterpretation problem. Literature [28] proposes to evaluate sleep status by placing pressure sensors under the mattress and perform signal processing through analyzing the pressure sensor signal, collecting the heart rate and turning over events, combining time variation and regression model of the feature extractor to obtain relevant features and parameters, and finally using the hidden Markov model (HMM) for sleep stage classification. An accuracy rate of 75% can be obtained in [28], which manifestly shows the problem of classification accuracy. Literature [29] proposes to use the time derivative of indentation in the mattress to detect turning over, while the pressure distribution image of mattress provides the basis for sleep posture assessment. When detecting that the subject has turned over, the algorithm would first extract the feature vector of the pressure image, and then, the feature vector is fed into SVM for sleep posture recognition. The experimental results show that the recognition rate of turning over detection can reach 91.2% and that of various postures can reach 83.6%–95.9%.

Literature [30] uses PPG and a pressure sensor placed under pillow for physiological signal monitoring and sleep posture detection; the PPG is used to detect HRV, and the pressure sensor is used to detect turning over action, through which to estimate the subject's sleep stage. The PPG sensor in this literature is placed on the wrist; as such, it is easily disturbed by turning over during sleep; and the measurement error is large. In addition, the use of pressure sensor placed under the pillow for determining to turn over is prone to being affected by slight head movement interference, and it is easy to cause misinterpretation of turning over.

In addition to the aforementioned approaches, some of the studies applied the use of wireless technology to detect the user's sleep posture and turnover activity, which eliminates the inconvenience of wearing a sensor device and allows the user or subject to be monitored in the most natural sleep condition without invading privacy [35], [36], among which a so-called "BodyCompass" system that is based on radio frequency technology is proposed to monitor the user's sleep posture in a wireless and noncontact manner [35]. The BodyCompass disentangles RF signals that bounced off the subject's body from other multipath signals to get the filtered profile features, and then, a multilayer fully connected neural network will be applied for the recognition of four kinds of sleep postures, including supine, left side, right side, and prone. With the one-week labeled data, the BodyCompass can have a classification accuracy up to 94.1%. Two noteworthy things are that BodyCompass provides not only the user's sleeping posture but also the rotation angle of the user with respect to the mattress since it estimates the angle between the normal vector of the user's anterior trunk surface and that of the bed surface. In addition, BodyCompass provides transfer learning capability based on the pretrained model for different users in their respective home environments so that the model can adapt itself to different environment and maintain a very good classification performance through small sample learning in new environments.

In [36], a SleepPoseNet is proposed for sleep posture transition recognition using UWB radar. The UWB is invoked for its capability of providing higher resolution range information due to high-frequency pulse signals [36]. The SleepPoseNet is basically composed of a deep CNN (DCNN) and multiview learning (MVL) architecture, and the SleepPoseNet first calculates the time difference (TD) in time domain and the weighted range–time–frequency transform (WRTFT) in frequency domain as the input features of the classifier, i.e., network inputs. With the MVL and DCNN, the SleepPoseNet is able to detect four kinds of posture transition, including supine to side (SUSI), supine to prone (SUPR), side to supine (SISU), and prone to supine (PRSU), as well as background situation with a classification accuracy of 73.7% [36].

In order to design a wear-free system that is able to evaluate the users' sleep status and quality with higher resistance capability against environmental interference but with no privacy concerns, we propose in this article a pressure-sensor-based smart mattress architecture. The proposed smart mattress adopts pressure sensors evenly distributed at 8-cm intervals to form a pressure-sensing matrix of 20 (height) $\times$ 11 (width), and all pressure-sensing elements will be sequentially scanned and the pressure value will be collected and then transmitted to the computer for analysis of the subject's sleep status and quality, which is convenient for home use and suitable for long-term sleep quality monitoring. In this article, SVM is used for sitting and lying posture recognition to evaluate the subjects' time in bed. Regarding sleep posture detection, four basic sleep postures can be classified by using the image formed by the pressure-sensing matrix in coordination with the proposed CNN model. With respect to sleep quality assessment, we adopt a set of four predefined parameters as fuzzy input variables to reckon the subject's sleep quality after fuzzification, fuzzy inference, and defuzzification. Compared

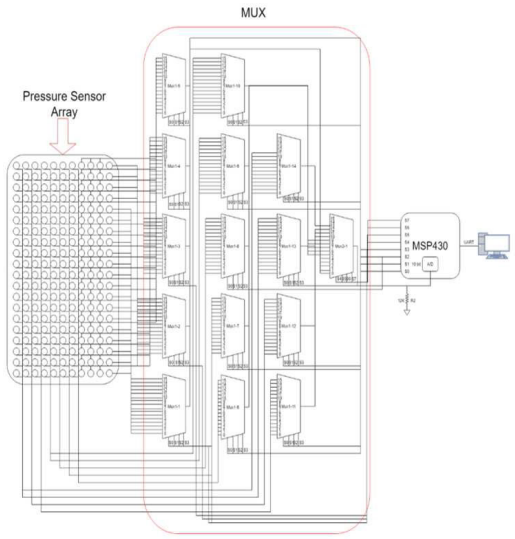

Fig. 1. Proposed hardware architecture.

with the foregoing literature, the proposed system does not need any wearable device, and as such, the subjects can complete the sleep quality detection in a natural and comfortable environment. This proposed system can provide relevant sleep parameters, including time in bed, number of times of bed leaving, number of times of body movements all night, standard deviation of time interval between body movements, as well as sleep posture, and finally provide the subject's sleep quality assessment report through a fuzzy inference algorithm. The sleep parameters collected by this system will be provided and used as a reference for physicians to evaluate sleep quality.

This article consists of five sections, and the contents of the remaining sections are given as follows. Section II explains the hardware and software architecture of the proposed system. The system algorithm, including how to form a pressure distribution image by means of the pressure-sensing matrix, how to use the SVM for sleep detection, how to conduct sleep posture detection in cooperation with CNN, as well as how to use fuzzy rules and various sleep parameters to carry out fuzzy inference and defuzzification to evaluate sleep quality, will be introduced in Section III. In Section IV, the experimental results on the performance of the proposed system and prior arts will be compared. Finally, Section V gives the conclusion of this article.

II. System Overview

Fig. 1 shows the hardware structure of the proposed pressure-sensor-based smart mattress system. The Texas Instruments (TI) MSP430G2553 microcontroller is used as the core of the smart mattress, scanning and collecting the pressure sensor values of each node on the mattress one by one through a two-level analog MUX and transmitting the values of each sensor node to the PC host via Universal Asynchronous Receiver and Transmitter (UART) interface to analyze whether the subject is sitting or lying on the mattress. In the event of lying on the mattress, further analysis of the user's sleep posture (including sleeping face up, lying face down, sleeping face left, and sleeping face right), time in bed, number of times of bed leaving, number of times of body movements all night, standard deviation of the time interval between body movements, and the pressure distribution of various sleep postures will be calculated, which finally combine with fuzzy rules and the information fed back by the subjects so as to proceed with sleep quality assessment and other reckons.

Fig. 2. Resistive pressure sensor in the proposed smart sensing matrix.

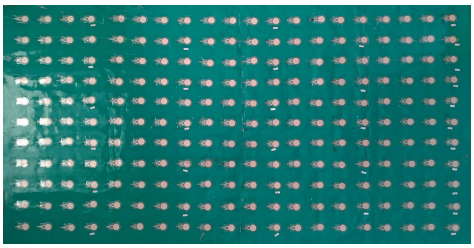

Fig. 3. Proposed 20 (height) × 11 (width) pressure-sensing matrix.

A. Hardware Architecture

In this article, we apply the GD25-100 N, a flexible resistive element provided by Uneo Inc., for pressure sensing (the element with two endpoints as shown in Fig. 2) [37]. The equivalent resistance value between the two endpoints is nearly infinite (i.e., similar to open circuit) when the sensing element is not squeezed; on the contrary, when the pressure is larger, the resistance value of the sensing element is smaller. We distribute the pressure sensors evenly on a soft pad with a length of 185 cm and a width of 95 cm and with an interval of 8 cm to form a 20 × 11 matrix with 220 nodes (as shown in Fig. 3), and then, the microcontroller will sequentially scan and obtain the value of each pressure-sensing node via the MUX to form a pressure distribution image.

Some of the important parameters of the GD25-100 N pressure sensor are listed as follows [37]:

1) linearity exceeding 99% over 0 to 100 N;
2) capable of up to 10 million actuations;
3) wide temperature range from −40 °C to 65 °C;
4) response time 0.1 ms (max).

B. Software Architecture

The sequentially scanned 20 × 11 pressure distribution image will be used for various user behavior analyses. In this article, we use an SVM in cooperation with this pressure image to analyze whether the subject is sitting or lying on a mattress, as well as calculate the user's time in bed. If it is determined that the subject is lying on the mattress, a proposed CNN model is further applied to commence sleep posture detection and turning over detection. As to sleep quality assessment, the fuzzy inference will be used, and a set of four predefined sleep parameters will be used as the fuzzy input variables to reckon the subject's sleep quality after fuzzification, fuzzy inference, and defuzzification.

The software interface of the proposed system is shown in Fig. 4. The system updates the scanned results at a frequency of 1 Hz. In addition, we divide the pressure values into

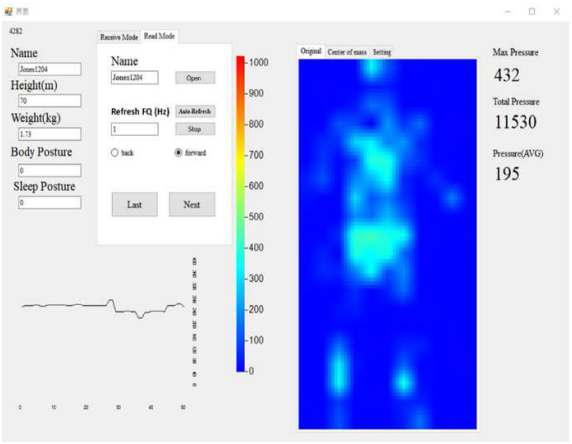

Fig. 4. Proposed software interface for pressure-sensing matrix data collection.

1024 levels (represented by 10 bits), and the nodes with higher pressures are displayed in warm colors (yellow and red), while cool colors (green and blue) are presented in contrast thereto. We can instantly know whether the user is sitting or lying on the mattress with this interface (when the column value corresponding to the body posture is 0, it means that the user is sitting on the mattress; otherwise, it means lying on the mattress). If it is confirmed that the user is lying on the mattress, we can further check the user's sleep posture via this interface (when the column value corresponding to sleep posture is 0, it means that the user is lying on your back (face up). If it is 1, it means sleeping on your right side (face right); if it is 2, it means lying on your left side (face left); if it is 3, it means lying on your stomach (face down). The bottom-left corner of Fig. 4 is the average pressure of each node in the last 50 s (i.e., 50 frames), and its value reflects the user's possible posture (sitting, lying, or on the side) to some extent.

1) Color Pressure Distribution Conversion: As aforesaid, the pressure value of each node returned by the microcontroller is between 0 and 1023 (a total of 1024 levels). To make the pressure distribution appear in a natural visual image, we can display the nodes with higher pressures in warm colors, but cool colors in contrast thereto as stated in (1). To do this, the RGB color model is adopted

$$\begin{cases} R = 0 \\ G = p_{ij} \times \dfrac{255}{\frac{1}{3}P_{\max} - 1}, & p_{ij} \le \dfrac{1}{3}P_{\max} \\ B = 255 \\ R = p_{ij} \times \dfrac{255}{\frac{1}{3}P_{\max} - 1} \\ G = 255, & \dfrac{1}{3}P_{\max} < p_{ij} \le \dfrac{2}{3}P_{\max} \\ B = 255 - \dfrac{\left(p_{ij} - \frac{1}{3}P_{\max}\right) \times 255}{\frac{1}{3}P_{\max} - 1} \\ R = 255 \\ G = 255 - \dfrac{\left(p_{ij} - \frac{1}{3}P_{\max}\right) \times 255}{\frac{1}{3}P_{\max} - 1}, & \dfrac{2}{3}P_{\max} < p_{ij} \le P_{\max} \\ B = 0 \end{cases} \tag{1}$$

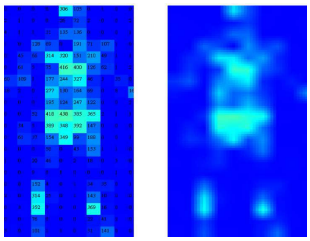

Fig. 5. Enlargement and smoothing of face-up pressure image. (a) Image after enlargement of elements. (b) Image after Gaussian low pass filtering.

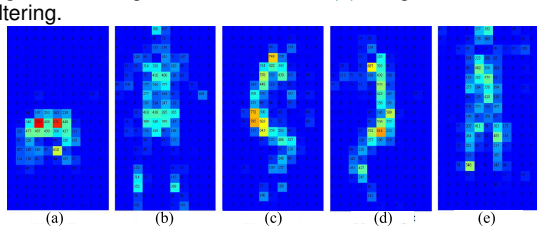

Fig. 6. Pressure image corresponding to the five different body postures after enlargement of elements. (a) Sitting. (b) Face up. (c) Face left. (d) Face right. (e) Face down.

where $P_{\max}$ in (1) is the maximum pressure and p_{ij} is the current pressure of the node in the ith row and jth column.

It can be seen from (1) that we divide the pressure value into three levels; we map $P_{\max}$ onto the maximum red color gradient in pressure distribution during the display process to highlight the pressure difference and enhance the contrast. When the pressure value is less than 1/3 $P_{\max}$, the component of R is fixed at 0, the component of B is fixed at 255, and the value of the green G is adjusted to change the color displayed. When the pressure value is between 1/3 $P_{\max}$ and 2/3 $P_{\max}$, the component of G is fixed at 255, and the values of blue B and red R are to be adjusted to change the color displayed. Finally, when the pressure value is between 2/3 $P_{\max}$ and $P_{\max}$, the component of R is fixed at 255, the component of B is fixed at 0, and the value of the green G is adjusted to change the color displayed.

2) Pressure Image Smoothing: Since the size of the original pressure image is 20 × 11, with a total of 220 nodes, the pressure image is subject to blocking effect, which is not visually intuitive and not conducive to the subsequent posture recognition. Therefore, we increase the number of picture elements (pixel) for the original pressure image (enlarge the original element to 6 × 6), and then, a Gaussian filter is applied for low-pass filtering (i.e., smoothing) on the image with an increased number of pixels. Fig. 5(a) shows the pressure image of face-up sleep posture after enlargement of elements, and Fig. 5(b) shows the image after low-pass Gaussian filtering (only enlargement and low-pass filtering is performed, without promoting the node with maximum pressure value to show in red). In this article, the mask size of the Gaussian low-pass filter used is 5 × 5, and the standard deviation σ is set to 2.7. Fig. 6 shows the pressure image of the subject's five body postures after enlargement of elements, and Fig. 7 shows the result of Fig. 6 after Gaussian smoothing.

III. Posture Detection and Sleep Quality Estimation

In this section, the proposed algorithm, including image preprocessing, determination of sitting and lying postures,

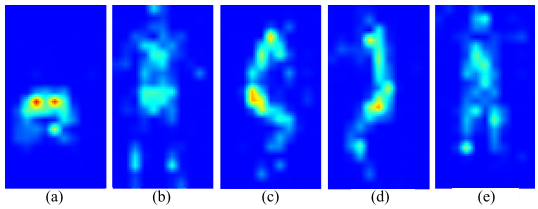

Fig. 7. Pressure image of the five postures in Fig. 6 after Gaussian smoothing. (a) Sitting. (b) Face up. (c) Face left. (d) Face right. (e) Face down.

TABLE I
CUMULATED WEIGHT RATIO AND CORRESPONDING PRESSURE VALUE OF THE FIVE POSTURES

Cumulated Weight Ratio / Body Posture	99%	98%	97%	96%	95%	94%	93%	92%	91%
Face Up	10.08	19.52	26.97	33.76	40.44	46.92	53.35	58.79	63.78
Face Right	10.62	21.84	31.36	40.25	49.89	58.68	67.14	75.33	82.82
Face Left	10.63	22.66	31.66	41.79	51.10	59.14	66.69	73.42	80.27
Face Down	10.94	23.16	32.76	42.22	50.09	57.23	64.34	70.73	76.88
Sitting	8.22	22.65	34.80	47.09	60.58	72.10	83.69	95.96	104.73
Average	10.10	21.97	31.51	41.02	50.42	58.82	67.04	74.84	81.70

sleep posture recognition, and sleep quality estimation, will be introduced.

A. Image Preprocessing

The preprocessing here is divided into three steps, including pressure threshold setting, differences between sitting and lying postures, and affine transformation of pressure image.

1) Pressure Threshold Setting: When the test subject is lying on the pressure-sensing mattress, the proposed system can detect the pressure distribution on each part of the mattress and display the pressure distribution image of the test subject. However, even if there is no subject on the mattress, the pressure sensor on the mattress might return a nonzero value of the pressure due to various factors, which is called noise interference; hence, the system needs to filter out such noise.

To filter out such noise interference, we test with 18 subjects and collect data on the five types of body postures from each subject, including sitting, lying face up, face right, face left, and lying face down; 1800 pieces of data are collected for each subject's aforesaid postures, and 9000 pieces of data are collected for the five types of body postures. We then extract 450 pieces of data for each of the four lying postures from the overall data collected to form 1800 pieces of lying posture data and further extract 1800 pieces of sitting posture data to form a total of 3600 pieces of sitting and lying posture data; the pressure image of the data is converted into a histogram, which is then scanned successively from the right side of the histogram (i.e., the one with higher pressure) to the left side (the one with lower pressure). The pressure values are accumulated in sequence, and the cumulated pressure value is divided by the pressure summation of the entire image, and after that, the cumulative weight ratio of the pressure value is obtained.

In this article, the pressure distribution of the foregoing five postures and the cumulated weight ratio from 91% to 99% is calculated, as shown in Table I and Fig. 8. We notice from Table I and Fig. 8 that the cumulated weight ratio of pressure

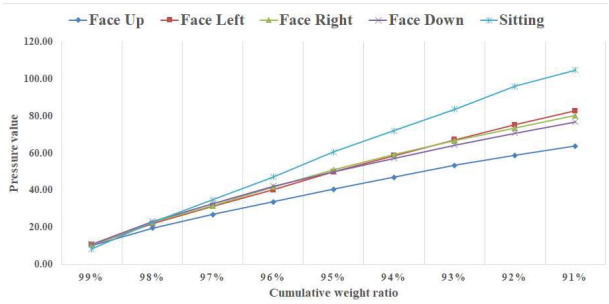

Fig. 8. Diagram of cumulated weight ratio corresponding to Table I.

value of various postures tends to be converged between 98% and 99%, while it is scattered between 98% and 91%, which shows that the pressure value corresponding to cumulated weight ratio of 98% is resulted by actual pressure of various postures. Therefore, we use the pressure value corresponding to the cumulated weight ratio 98% (i.e., 21.97) as the denoising threshold (P_θ). We then set the pressure value lower than the threshold value P_θ to be 0 and keeps pressure readings equal to or greater than this threshold unchanged, as in the following equation:

$$\widetilde{p}_{ij} = \begin{cases} p_{ij}, & \text{if } p_{ij} > P_\theta \\ 0, & \text{otherwise} \end{cases} \tag{2}$$

where P_θ is set to be 22 (i.e., a rounded value of 21.97) in this article.

2) Features Extraction and Classification for Sitting and Lying Postures: To recognize whether the user is lying on the mattress or sitting on the mattress, an SVM will be applied for the classification process. For this, we use five features captured from the pressure image as the feature vector of the SVM. With an off-line training process, the SVM is capable of recognizing sitting and lying postures. The following are the extraction methods of the five features.

1) The first feature is the average pressure value of the pressure image. When the subject is sitting on the bed, the contact area between the subject and the mattress is smaller than that of lying in bed; thus, the average pressure when the subject sits on the mattress will be greater than that when the user is lying in bed; the average pressure is calculated as that in the following equation:

$$\bar{P} = \frac{\sum_i \sum_j \widetilde{p}_{\mathrm{ij}}}{n} \tag{3}$$

where n is the number of pressure sensors with pressure value greater than P_θ and $\widetilde{P}_{ij}$ is the current pressure value of the node in the ith row and jth column after the threshold denoising in (2).

2) The second feature is the variation in pressure sensor readings. We may find that the variation of each pressure reading corresponding to lying down is obviously greater than that of sitting posture. Thus, the variation of the readings of the nonzero pressure sensors on the mattress, such as (4), may be used as one of the features to

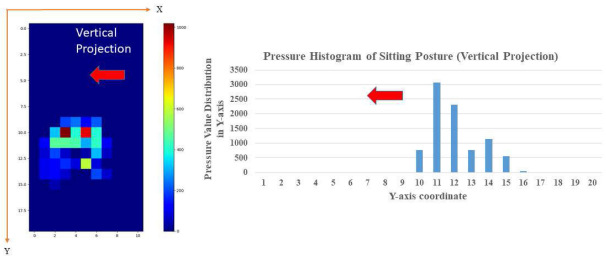

Fig. 9. Sitting pressure distribution image and the histogram of pressure projected onto vertical axis.

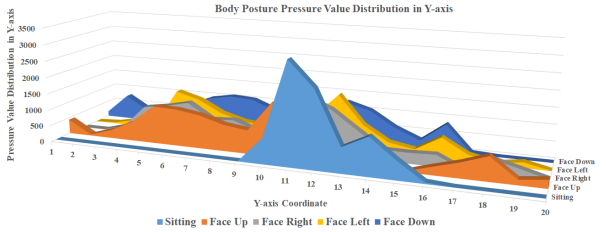

Fig. 10. Projected pressure distribution of various postures on vertical axis.

differentiate sitting and lying postures

$$\sigma_P^2 = \frac{\sum_i \sum_j \left(\widetilde{p}_{ij} - \bar{P}\right)^2}{n} \tag{4}$$

where σ_P^2 is the variance feature of the histogram and n is identical as that in (3).

3) The third feature is the pressure distribution variation of the image on the vertical axis (Y-axis). We project the pressure image on the vertical axis (Y-axis), calculate its histogram, and observe the pressure distribution image on the histogram (Figs. 9 and 10), and it is found that compared with the pressure images of lying posture (including lying face up, face right, face left, and lying face down), the dispersion degree of the pressure histogram corresponding to sitting posture on the Y-axis is significantly smaller. Thus, the variance (7) on the histogram after projecting on the Y-axis (i.e., the vertical axis) can be used as one of the features to differentiate between sitting and lying postures. To do this, we first calculate the accumulated pressure P_{Sum} of the image as follows:

$$P_{\text{Sum}} = \sum_{j=1}^{Y} \sum_{i=1}^{X} \widetilde{p}_{ij} \tag{5}$$

where $X = 11$, $Y = 20$ in this article, and $\widetilde{p}_{ij}$ is the pressure sensor reading after threshold processing in (2). We then calculate y_c, i.e., the center of gravity of the pressure image for Y-axis, as follows:

$$y_c = \frac{\sum_{j=1}^{Y} \left(\sum_{i=1}^{X} \widetilde{p}_{ij}\right) j}{P_{\text{Sum}}} \tag{6}$$

where j is the coordinate position on the Y-axis. Finally, the pressure distribution variation of the image on the vertical axis (Y-axis), i.e., σ_Y^2, can be obtained in the following equation:

$$\sigma_Y^2 = \frac{\sum_{j=1}^{Y} \left(\sum_{i=1}^{X} \widetilde{p}_{ij}\right) (j - y_c)^2}{P_{\text{Sum}}}. \tag{7}$$

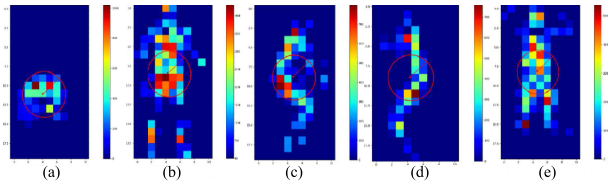

Fig. 11. To find an appropriate radius of the circle located in the gravity of pressure image to distinguish sitting and the four lying postures. (a) Sitting. (b) Face up. (c) Face left. (d) Face right. (e) Face down.

4) The fourth feature is the ratio of the cumulated pressure within a circle (with center in the gravity) with respect to the entire sheet of pressure image (i.e., percentage of pressure within the circle). Obviously, a larger ratio can be expected for a sitting posture than that for lying postures. For this, we have to find an appropriate radius for this circle. We first calculate that the center of gravity of the pressure image (the gravity center on the vertical axis (Y-axis) is calculated in (6) and that of the horizontal axis (X-axis) is calculated in the following equation:

$$x_c = \frac{\sum_{i=1}^{X} \left(\sum_{j=1}^{Y} \widetilde{p}_{ij}\right) i}{P_{\text{Sum}}} \tag{8}$$

where i is the coordinate position on the X-axis and x_c is the barycentric coordinate of the pressure image for X-axis.

With the gravity center determined, we then expand the radius outward gradually by 1 pixel at a time (as shown in Fig. 11) and then calculate the ratio of the entire pressure within the circle formed under each radius and the entire sheet of pressure image. Fig. 12 shows the resulting variation with 200 pieces of data collected, including 100 pieces of sitting posture data, and the other 100 pieces of data including 25 pieces of each posture such as lying face up, face right, face left, and lying face down. We can see in Fig. 12 that when the radius is 3 pixels, the average percentage of pressure within the circle of sitting posture is 0.889 (i.e., 88.9%), while the average pressure ratio within the circle of lying posture is 0.4571 (i.e., 45.71%), a maximal percentage of difference between sitting and lying postures can be obtained. Therefore, the optimal radius value to differentiate between sitting and lying postures is 3 pixels.

5) The fifth feature is the percentage of the number of pressure sensors in the circle formed by a given radius. To do this, we have to find the most suitable radius to distinguish between sitting and various lying positions. We first use the center of gravity of the pressure image as the center of the circle and increase the radius by 1 pixel each time, as shown in Fig. 11. We calculate

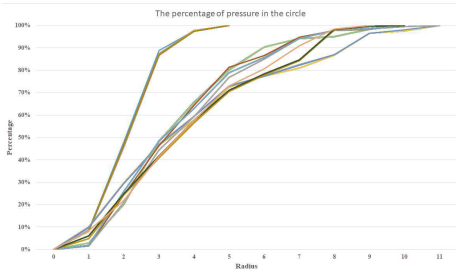

Fig. 12. Percentage of pressure in the circle formed by the increasing radius to the total image pressure value.

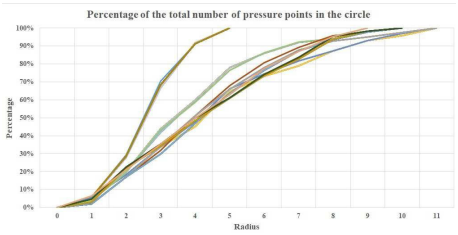

Fig. 13. Percentage of points in the circle formed by the increasing radius to the total number of sensor nodes with value greater than P_θ.

the percentage of the total number of pressure sensors in the circle formed by different radii to the total number of pressure sensors in the entire pressure image. The statistical result is shown in Fig. 13. The data used in Fig. 13 are the same as that in Fig. 12, i.e., 200 data of different postures are used, including 100 sitting posture data, and the other 100 data include face up, face right, face left, and face down, each with 25 data. As can be seen from Fig. 13, when the radius is 3 pixels, the average percentage of the number of sensors in the circle corresponding to sitting posture is 68% and that corresponding to lying postures is 36%. A maximal percentage difference can be obtained at this time. Therefore, we choose the optimal radius to distinguish between sitting and lying postures to be 3 pixels.

Finally, we used a set of 3600 training data, including 1800 sitting postures and 1800 lying postures, to calculate the aforementioned five features. These features are then applied for the training of an SVM to establish a model for sitting and lying postures identification.

3) Translation and Rotation of Pressure Images: In this section, we will explain the preprocessing flow for lying postures recognition. When the subject is lying on the mattress, it is not necessarily right in the middle of the mattress, and the main trunk of the body is not necessarily perpendicular to the horizontal axis of the mattress, which will affect the accuracy of the sleeping posture recognition and lead to a higher complexity in model training. Therefore, when performing sleep posture recognition, we will first perform translation and rotation on the pressure image, i.e., the affine transformation will be performed, so that the user's pressure image is located in the center of the mattress and that of the main trunk is perpendicular to the horizontal axis (Y-axis) of the mattress. This will reduce the amount of data required for model training

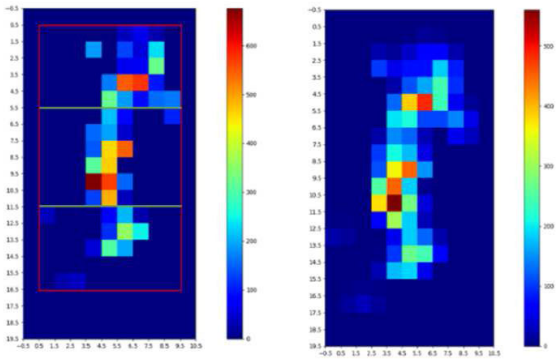

Fig. 14. Pressure images before and after translation. (a) Before translation. (b) After translation.

while improving the accuracy of sleep postures recognition. To do this, the following steps will be performed.

Step 1: First, we find the enclosing rectangle of the user's pressure image [as the red frame in Fig. 14(a)] and equally divide the rectangle into three parts vertically [as the horizontal green frame in Fig. 14(a)]. We then calculate the average pressure inside the upper and lower intervals. The one with a larger average pressure is the upper body and that with smaller average pressure is the lower limbs. If the subject's head is at the tail of the mattress, the system will automatically rotate the pressure image.

Step 2: In the proposed system, the gravity center (c_x, c_y) of the user's pressure image will be located in the coordinate (5, 10). Therefore, the amount of horizontal and vertical translation t_x and t_y can be determined based on (9) and (10), respectively.

$$t_x = 5 - x_c \tag{9}$$

$$t_y = 10 - y_c \tag{10}$$

where x_c and y_c are the coordinate of horizontal and vertical gravity center in (8) and (6), respectively. With the translation calculated in (9) and (10), we can construct a translation matrix $T_r(t_x, t_y)$ in (11), and the translated pressure image can be obtained by multiplying the original pressure image with the translation matrix [the resulted image is shown in Fig. 14(b)]

$$T_r(t_x, t_y) = \begin{bmatrix} 1 & 0 & t_x \\ 0 & 1 & t_y \\ 0 & 0 & 1 \end{bmatrix}. \tag{11}$$

Step 3: After the image has been translated to the center of the mattress, the next step is to rotate the image so that the main trunk of the subject's pressure image is perpendicular to the horizontal axis (X-axis). In the first step, we divided the pressure image into three equal sections, and here, we calculate the gravity center of the upper body section and that of the middle section in the pressure image. We then connect the gravity center of the upper body toward that of the middle section to form a vector $\vec{a}$. In addition, we take the positive direction of the vertical axis (i.e., Y-axis) of the mattress as the

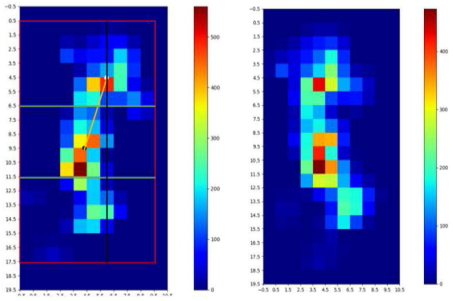

Fig. 15. Pressure images before and after rotation. (a) Before rotation. (b) After rotation.

vector $\vec{b}$ and use the inner product to calculate the angle between vector $\vec{a}$ and $\vec{b}$ as in (12), which corresponds to the angle of rotation

$$\theta = \cos^{-1} \frac{\vec{a} \cdot \vec{b}}{|\vec{a}| \left|\vec{b}\right|}. \tag{12}$$

With θ calculated in (12), a rotation matrix can be obtained in the following equation:

$$R(\theta) = \begin{bmatrix} \cos\theta & -\sin\theta & 0 \\ \sin\theta & \cos\theta & 0 \\ 0 & 0 & 1 \end{bmatrix}. \tag{13}$$

Step 4: It is noted that the coordinate ($c_x = 5$, $c_y = 10$), i.e., center of the mattress, should be used as the center of rotation since the gravity center of the pressure image has been translated to (5, 10). However, the rotation matrix in (13) takes the origin (0, 0) as the center of rotation. Hence, we have to offset the coordinate of gravity to the origin beforehand and then offset the gravity of the image back to the center of the mattress, i.e., ($c_x = 5$, $c_y = 10$). For this, an overall operation can be obtained in the following equation:

$$\begin{aligned} &T_r(c_x, c_y) R(\theta) T_r(-c_x, -c_y) \\ &\quad = \begin{bmatrix} \cos\theta & -\sin\theta & c_x(1-\cos\theta) + c_y \sin\theta \\ \sin\theta & \cos\theta & c_y(1-\cos\theta) - c_x \sin\theta \\ 0 & 0 & 1 \end{bmatrix}. \end{aligned} \tag{14}$$

After applying the overall transformation, a rotated pressure image of the subject can be obtained, as shown in Fig. 15(b).

B. Sleep Postures Recognition

This article uses CNN for sleep postures recognition, as shown in Fig. 16. The proposed CNN can be roughly classified as the former convolutional layer and the latter classification layer (a fully connected network); the convolutional layer is used to generate the corresponding features and then proceed with classification for sleep postures recognition by means of the latter classification layer.

As shown in Fig. 16, we use two convolutional layers and one max-pooling layer for feature extraction in this article. Max pooling effectively overcomes the misrecognition of the classifier caused by slight image translation and rotation. The original image generates a feature map through the convolution layer, and the rectified linear unit (ReLU) activation function is used to convert the negative value of the convolution result to 0. The flatten operation after pooling can form a single-dimensional array, which is then delivered into the subsequent classification layer, and the classification layer adopts a fully connected layer; as such, all the neuron nodes can vote on the result.

In this article, four basic sleep postures are to be recognized: face up, face right, face left, and face down. The system uses 36 000 sample data for model training, and the trained network shows a recognition accuracy up to 96.987% in the subsequent sleep postures test all night long. It appears obvious that the proposed system can achieve the function correctly recognizing sleep postures.

C. Sleep Quality Assessment

To assess sleep quality, the fuzzy inference is applied in this article. As shown in Fig. 17, the fuzzy inference system includes three parts: defining the membership function (fuzzification), fuzzy rules, and defuzzification. The left of Fig. 17 is the four parameters used for sleep quality assessment in this article. Such sleep quality parameters are first fuzzified by means of the membership function, combined with fuzzy rules to make fuzzy inferences, and finally, the sleep quality is estimated by using defuzzification.

In this article, a membership function is determined based on experience, and the four sleep quality parameters are used to define the input membership function as follows:

1) time in bed;
2) number of times of bed leaving;
3) number of times of body movements (or turning over) all night;
4) standard deviation of the interval between body movements.

The membership functions of the four indicators listed above are shown in (15)–(17), (18) and (19), (20)–(22), and (23) and (24), respectively. Among them, $\mu_1(x_1)$, $\mu_2(x_2)$, $\mu_3(x_3)$, and $\mu_4(x_4)$ are the membership functions of time in bed, number of times of bed leaving, number of times of body movements all night, and standard deviation of the interval between body movements, respectively. In addition, the diagrams of the membership functions are shown in Fig. 18(a)–(d).

Turning over is the body's self-protection mechanism, which can reduce the risk of pressure ulcers. However, excessive turning over will make it difficult for people to enter deep sleep, and the overall sleep quality will decrease [38]. Therefore, the number of body movement or turning over is included as one of the sleep quality evaluation indicators

$$\mu_1^L(x_1) = \begin{cases} 1, & x_1 < 5 \\ (7 - x_1)/2, & 5 \le x_1 < 7 \\ 0, & x_1 \ge 7 \end{cases} \tag{15}$$

$$\mu_1^H(x_1) = \begin{cases} 0, & x_1 < 9 \\ (x_1 - 9)/2, & 9 \le x_1 < 11 \\ 1, & x_1 \ge 11 \end{cases} \tag{16}$$

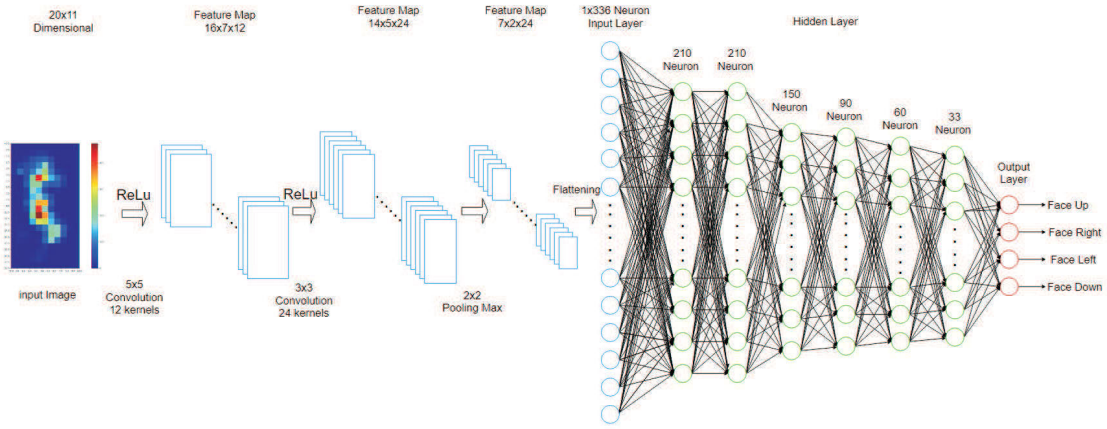

Fig. 16. Proposed CNN architecture for sleep postures recognition.

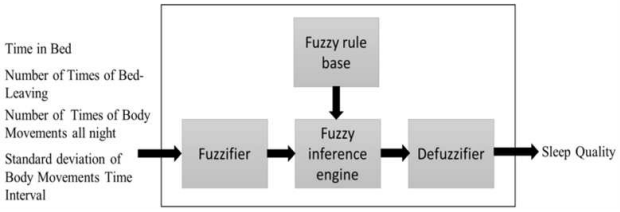

Fig. 17. Fuzzy system architecture and parameters used for sleep quality assessment.

$$\mu_1^H(x_1) = \begin{cases} 0, & x_1 < 9 \\ (x_1 - 9)/2, & 9 \le x_1 < 11 \\ 1, & x_1 \ge 11 \end{cases} \tag{17}$$

$$\mu_2^L(x_2) = \begin{cases} 1, & x_2 < 1 \\ 4 - x_2, & 1 \le x_2 < 4 \\ 0, & x_2 \ge 4 \end{cases} \tag{18}$$

$$\mu_2^H(x_2) = \begin{cases} 0, & x_2 < 1 \\ x_2 - 1, & 1 \le x_2 < 4 \\ 1, & x_2 \ge 4 \end{cases} \tag{19}$$

$$\mu_3^L(x_3) = \begin{cases} 1, & x_3 < 10 \\ (35 - x_3)/25, & 10 \le x_3 < 35 \\ 0, & x_3 \ge 35 \end{cases} \tag{20}$$

$$\mu_3^M(x_3) = \begin{cases} 0, & x_3 < 10 \\ (x_3 - 10)/25, & 10 \le x_3 < 35 \\ (60 - x_3)/25, & 35 \le x_3 < 60 \\ 0, & x_3 \ge 60 \end{cases} \tag{21}$$

$$\mu_3^H(x_3) = \begin{cases} 0, & x_3 < 35 \\ (x_3 - 35)/25, & 35 \le x_3 < 60 \\ 1, & x_3 \ge 60 \end{cases} \tag{22}$$

$$\mu_4^L(x_4) = \begin{cases} 1, & x_4 < 10 \\ (40 - x_4)/30, & 10 \le x_4 < 40 \\ 0, & x_4 \ge 40 \end{cases} \tag{23}$$

$$\mu_4^H(x_4) = \begin{cases} 0, & x_4 < 10 \\ (x_4 - 10)/30, & 10 \le x_4 < 40 \\ 1, & x_4 \ge 40. \end{cases} \tag{24}$$

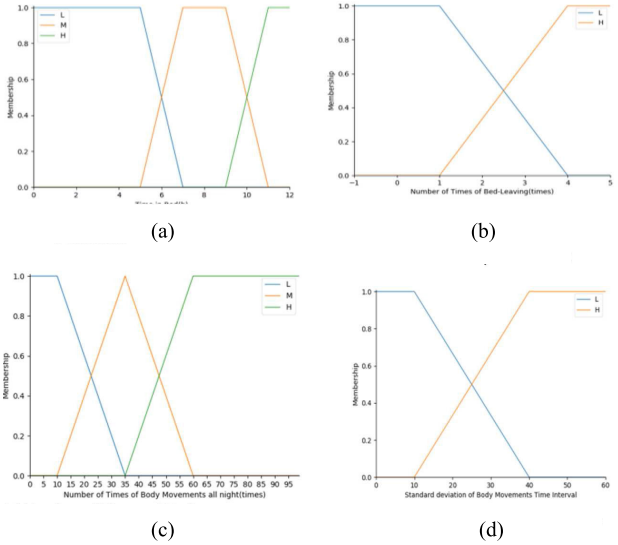

Fig. 18. Membership functions of sleep quality parameters. (a) Time-in-bed membership function. (b) Number-of-times-of-bed-leveling membership function. (c) Number-of-times-of-body-movements-all-night membership function. (d) Standard-deviation-of-body-movements-time-interval membership function.

The 24 fuzzy rules in this article are shown in Table II. Moreover, the corresponding output membership functions and diagrams are shown in (25)–(29) and Fig. 19, respectively

$$\mu_5^{\text{Very Bad}}(x_5) = \begin{cases} 1, & x_5 < 20 \\ (35 - x_5)/15, & 20 \le x_5 < 35 \\ 0, & x_5 \ge 35 \end{cases} \tag{25}$$

$$\mu_5^{\text{Bad}}(x_5) = \begin{cases} 0, & x_5 < 20 \\ (x_5 - 20)/15, & 20 \le x_5 < 35 \\ (50 - x_5)/15, & 35 \le x_5 < 50 \\ 0, & x_5 \ge 50 \end{cases} \tag{26}$$

$$\mu_5^{\text{Fair}}(x_5) = \begin{cases} 0, & x_5 < 35 \\ (x_5 - 35)/15, & 35 \le x_5 < 50 \\ (65 - x_5)/15, & 50 \le x_5 < 65 \\ 1, & x_5 \ge 65 \end{cases} \tag{27}$$

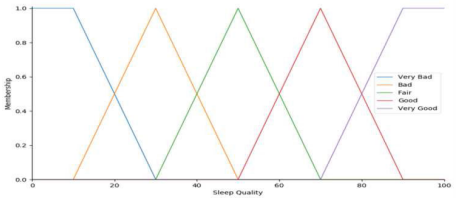

Fig. 19. Output membership functions.

TABLE II
FUZZY RULES FOR SLEEP QUALITY EVALUATION

Rule Number	Time in Bed	Number of Times of Bed-Leaving	Number of Times of Body Movements all night	Standard deviation of Body Movements Time Interval	Sleep Quality
1	M	L	M	L	Very Good
2	L	L	M	L	Good
3	M	H	M	L	Good
4	M	L	L	L	Fair
5	H	L	M	L	Fair
6	M	L	M	H	Fair
7	L	L	M	H	Bad
8	L	H	M	L	Bad
9	M	L	L	H	Bad
10	M	H	L	L	Bad
11	M	H	M	H	Bad
12	H	H	M	L	Bad
13	L	L	L	×	Very Bad
14	L	L	H	×	Very Bad
15	L	H	L	×	Very Bad
16	L	H	M	H	Very Bad
17	L	H	H	×	Very Bad
18	M	L	H	×	Very Bad
19	M	H	L	H	Very Bad
20	M	H	H	×	Very Bad
21	H	L	L	×	Very Bad
22	H	×	M	H	Very Bad
23	H	×	H	×	Very Bad
24	H	H	H	×	Very Bad

$$\mu_5^{\text{Good}}(x_5) = \begin{cases} 0, & x_5 < 50 \\ (x_5 - 50)/15, & 50 \le x_5 < 65 \\ (80 - x_5)/15, & 65 \le x_5 < 80 \\ 0, & x_5 \ge 80 \end{cases} \tag{28}$$

$$\mu_5^{\text{Very Good}}(x_5) = \begin{cases} 0, & x_5 < 65 \\ (x_5 - 65)/15, & 65 \le x_5 < 80 \\ 1, & x_5 \ge 50. \end{cases} \tag{29}$$

In this article, the center-of-gravity method is applied for the process of defuzzification, as in the following equation:

$$g(k) = \frac{\int x_5 \mu_5^k(x_5) \mathrm{d}x_5}{\int \mu_5^k(x_5) \mathrm{d}x_5} \tag{30}$$

where $k \in \{\text{Very Bad, Bad, Fair, Good, Very Good}\}$, which indicates the sleep quality rating. In addition, the weight corresponding to the five levels of sleep quality is calculated according to the following equation:

$$w_k = \max_{1 \le l \le 24} \left[\min \left(\mu_{i,l}^k (x_i) \right) \right] \tag{31}$$

where $i \in \{1, 2, 3, 4\}$, which indicates the four sleep quality parameters, l and k are the rule number and sleep quality rating, respectively, and $\mu_{i,l}^k(x_i)$ is the excitation intensity of the kth sleep quality level in the lth rule. After that, the weighted average for sleep quality is calculated as in (32). Finally,

TABLE III
SCORE AND CORRESPONDING SLEEP QUALITY RATING

$f(z)$	0∼20	20∼40	40∼60	60∼80	80∼100
Sleep Quality	Very Bad	Bad	Fair	Good	Very Good

Table III is used to map sleep score onto the corresponding sleep quality

$$f(z) = \frac{\sum w_k g(k)}{\sum w_k}. \tag{32}$$

IV. EXPERIMENTAL RESULTS

A. Experimental Environment

In this article, the experiments are divided into two environments; the first scenario is a laboratory training environment and the second scenario is a home test environment. The laboratory environment is for classification model (including the SVM model for sitting and lying posture classification as well as the CNN model for four kinds of sleep postures recognition) training and performance validation, while the home environment is for models performance test. Moreover, the subject's pressure distribution will be collected continuously throughout the night during sleep and an IR camera will be used for recording as ground truth during the home test scenario.

In this article, the hardware specifications and system development environment are given as follows.

Hardware Facilities:

1) *Pressure-Sensing Mattress:* 185 × 95 cm.
2) *Number of Pressure-Sensing Elements:* 220 (i.e., 11 × 20).
3) *Pressure-Sensing Element:* UNEO GD10-20 N.
4) *Microcontroller:* TI MSP430G2553.

Software Development Tools:

1) *Firmware Development Environment:* Code Composer Studio 6.2.0.
2) *Software Development Environment:* Visual Studio 2017 and Sublime Text.
3) *Programming Languages:* C, C#, and Python.

B. Data Collection

As aforementioned, the data for classification model training (laboratory environment) and that for model test (home environment) is different and subject independent. A detailed description on the data collection process is given as follows.

1) Training Data Collection for Sitting and Lying Postures Recognition in Laboratory Environment: During the training data collection process in the laboratory environment, there are 18 test subjects (15 males and three females) between 22 and 29 years of age (average 24.2 ± 1.93 years) in our experiments, whose data are shown in Table IV. The test subjects are asked to do the following specified actions for pressure data collection.

1) *Sitting Posture [Fig. 20(a)]:* Full body relaxation, natural placement of hands and feet, and posture maintained for 100 s.

TABLE IV
DATA OF THE 18 SUBJECTS PARTICIPATED IN LABORATORY TRAINING

Subject ID	Age	Gender	Height(m)	Weight(Kg)	BMI
1	22	M	1.75	64	20.90
2	24	M	1.7	60	20.76
3	24	M	1.74	64	21.14
4	23	M	1.8	55	16.98
5	24	F	1.63	61	22.96
6	24	M	1.8	60	18.52
7	23	F	1.58	48	19.23
8	23	M	1.7	50	17.30
9	29	M	1.79	92	28.71
10	24	M	1.83	70	20.90
11	25	M	1.7	50	17.30
12	22	M	1.64	61	22.68
13	23	M	1.8	78	24.07
14	23	M	1.72	58	19.61
15	26	M	1.68	63	22.32
16	24	F	1.51	45	19.74
17	24	M	1.79	76	23.72
18	29	M	1.73	70	23.39

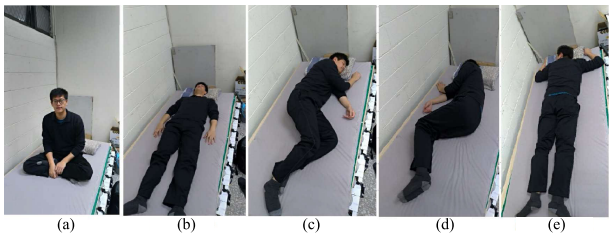

Fig. 20. Five postures for data collection. (a) Sitting. (b) Face up. (c) Face left. (d) Face right. (e) Face down.

2) *Lying Face Up [Fig. 20(b)]:* Full body relaxation, natural placement of hands and feet, and posture maintained for 100 s.
3) *Lying Face Left [Fig. 20(c)]:* Lying on the left side with both feet stretched or flexed, and posture maintained for 100 s.
4) *Lying Face Right [Fig. 20(d)]:* Lying on the right side with both feet stretched or flexed, and posture maintained for 100 s.
5) *Lying Face Down [Fig. 20(e)]:* Lying on the chest, full body relaxation, natural placement of hands and feet, and posture maintained for 100 s.

The sampling frequency of the mattress system is set to be 1 Hz (i.e., one record per second). Therefore, there are 100 pieces of posture data in each action and five types of body posture data are collected for each test subject. Therefore, 18 subjects created 1800 training data for each posture, and five postures can have 9000 training data in total. The data collected are used for the sitting and lying posture recognition (in Section III-A2) as well as the four lying postures recognition (in Section III-B) when the subjects are sleeping on the smart mattress. Moreover, since the model complexity of the CNN is higher than that of SVM, a data augmentation process is performed for the four different sleeping postures, bringing the total number of training data for the four sleeping postures to 36 000, so that the CNN model can be better trained.

2) Test Data Collection for Sleep Postures Recognition and Sleep Quality Analysis at Home Environment: There are two subjects (one male and one female) in the home test scenario. The personal physical data of the two subjects are shown in Table V. The age of the subjects is 29 (male) and 73 (female). During the test, the subjects sleep on the smart mattress all night to collect sleep data. In addition, a camera is set up to fully record the subject's posture during the experiment, including events such as turning over and getting up. In this article, data from a total of six nights of sleep are collected in the home scenarios, and each subject's data are collected from three nights of sleep.

TABLE V
DATA OF THE TWO SUBJECTS PARTICIPATED IN HOME TEST SCENARIO

Subject ID	Age	Gender	Height(m)	Weight(Kg)	BMI
1	29	Male	1.73	70	23.4
2	73	Female	1.50	46	20.4

C. Efficacy Evaluation of Various Posture Recognition and Sleep Quality Analysis

1) Sitting and Lying Posture Recognition: To evaluate the recognition accuracy between sitting and lying postures, the scenario of the two subjects at home is used for the experiment. The recognition results between sitting and lying postures for six nights are shown in Tables VI and VII, respectively. Among them, Table VI shows the detailed results per night, where Table VII gives a summary. In this experiment, a total of 153 307 s of data are collected in six nights. As can be seen in Table VII, the time of successful recognition is 153 285 s, and that of wrong recognition is 22 s. The accuracy rate is 99.986%. In this article, the sensitivity (33), specificity (34), precision (35), negative predictive value (NPV) [see (36)], F1 score (37), and accuracy (38) are used for the performance evaluation of classification. The performance indicators for the recognition of sitting and lying posture are shown in Table VIII. As can be seen in Table VIII, the classification performance of the proposed SVM classifier in sitting and lying positions recognition is satisfactory and reliable

$$\text{Sensitivity} = \frac{\text{TP}}{\text{TP} + \text{FN}} \tag{33}$$

$$\text{Specificity} = \frac{\text{TN}}{\text{FP} + \text{TN}} \tag{34}$$

$$\text{Precision} = \frac{\text{TP}}{\text{TP} + \text{FP}} \tag{35}$$

$$\text{NPV} = \frac{\text{TN}}{\text{FN} + \text{TN}} \tag{36}$$

$$\text{F1 Score} = \frac{2}{\frac{1}{\text{Precision}} + \frac{1}{\text{Recall}}} \tag{37}$$

$$\text{Accuracy} = \frac{\text{TP} + \text{TN}}{\text{TP} + \text{FP} + \text{FN} + \text{TN}} \tag{38}$$

where TP, TN, FP, FN represent true positive, true negative, false positive, and false negative, respectively.

2) Sleep Postures Recognition: In this experiment, the four lying postures of the two subjects at home test environment for six nights are used for performance evaluation. The results

TABLE VI
STATISTICAL RESULTS OF SITTING AND LYING POSTURES OF THE TWO SUBJECTS AT HOME TEST ENVIRONMENT FOR SIX NIGHTS (UNITS OF TIME IN SECONDS)

Subject ID	Real Posture / Predicted Result	Sitting Posture	Lying Posture	Total
1 (Day 1)	Sitting Posture	101	0	101
	Lying Posture	0	26,631	26,631
	Total	101	26,631	26,732
1 (Day 2)	Sitting Posture	116	0	116
	Lying Posture	0	24,545	24,545
	Total	116	24,545	24,661
1 (Day 3)	Sitting Posture	74	0	74
	Lying Posture	0	25,749	25,749
	Total	74	25,749	25,823
2 (Day 1)	Sitting Posture	64	0	64
	Lying Posture	3	24,720	24,723
	Total	67	24,720	24,787
2 (Day 2)	Sitting Posture	50	12	62
	Lying Posture	0	28,405	28,405
	Total	50	28,417	28,467
2 (Day 3)	Sitting Posture	103	3	106
	Lying Posture	4	22,727	22,730
	Total	107	22,730	22,837

TABLE VII
STATISTICAL SUMMARY (I.E., CONFUSION MATRIX) OF THE PROPOSED SVM MODEL FOR THE CLASSIFICATION OF SITTING AND LYING POSTURES OF THE TWO SUBJECTS AT HOME TEST ENVIRONMENT FOR SIX NIGHTS (UNITS OF TIME IN SECONDS)

Real Posture / Predicted Result	Sitting Posture	Lying Posture	Total
Sitting Posture	508	15	523
Lying Posture	7	152,777	152,784
Total	515	152,792	153,307

TABLE VIII
PERFORMANCE INDICATORS OF THE PROPOSED SVM MODEL FOR THE CLASSIFICATION OF SITTING AND LYING POSTURE AT HOME TEST ENVIRONMENT

Posture / Performance Index	Sitting Posture	Lying Posture
Sensitivity	98.64%	99.99%
Specificity	99.99%	98.64%
Precision	97.13%	100.00%
NPV	100.00%	97.13%
F1 Score	97.88%	99.99%
Accuracy	99.99%	

are shown in Tables IX and X. Table IX shows the detailed results of the proposed CNN model, and Table X gives a summary (i.e., confusion matrix) of the recognition results. As can be seen in Table X, a total of 152 792 s of lying posture data are collected in six nights. Among them, 148 189 s are successfully recognized, while 4603 s are misclassified. Thus, the proposed CNN model for lying postures recognition has an accuracy rate of 96.987%. In addition, the commonly

TABLE IX
STATISTICAL RESULTS OF SLEEP POSTURES OF THE TWO SUBJECTS AT HOME TEST ENVIRONMENT FOR SIX NIGHTS

Subject ID	Real Posture / Predicted Posture	Face Up	Face Right	Face Left	Face Down	Total
1 (Day 1)	Face Up	14,819	0	264	0	15,083
	Face Right	1,079	5,227	0	0	6,306
	Face Left	241	0	4,985	0	5,226
	Face Down	9	0	7	0	16
	Total	16,148	5,227	5,256	0	26,631
1 (Day 2)	Face Up	13,382	0	0	0	13,382
	Face Right	3	1,647	0	0	1,650
	Face Left	1,306	0	8,204	0	9,510
	Face Down	0	0	3	0	3
	Total	14,691	1,647	8,207	0	24,545
1 (Day 3)	Face Up	19,260	0	0	0	19,260
	Face Right	3	3,259	3	0	3,265
	Face Left	32	0	3,166	0	3,198
	Face Down	14	12	0	0	26
	Total	19,309	3,271	3,169	0	25,749
2 (Day 1)	Face Up	9,263	0	0	0	9,263
	Face Right	0	15,393	0	0	15,393
	Face Left	0	0	0	0	0
	Face Down	57	7	0	0	64
	Total	9,320	15,400	0	0	24,720
2 (Day 2)	Face Up	16,971	1,362	0	0	18,333
	Face Right	34	10,030	0	0	10,064
	Face Left	13	0	0	0	13
	Face Down	4	3	0	0	7
	Total	17,022	11,395	0	0	28,417
2 (Day 3)	Face Up	8,125	7	0	0	8,132
	Face Right	128	13,936	0	0	14,064
	Face Left	0	0	0	0	0
	Face Down	9	3	0	522	534
	Total	8,262	13,946	0	522	22,730

TABLE X
STATISTICAL SUMMARY (I.E., CONFUSION MATRIX) OF THE PROPOSED CNN MODEL FOR THE RECOGNITION OF THE FOUR SLEEP POSTURES OF THE TWO SUBJECTS AT HOME TEST ENVIRONMENT FOR SIX NIGHTS

Real Posture / Predicted Posture	Face Up	Face Right	Face Left	Face Down	Total
Face Up	81,820	1,369	264	0	83,453
Face Right	1,247	49,492	3	0	50,742
Face Left	1,592	0	16,355	0	17,947
Face Down	93	25	10	522	650
Total	84,752	50,886	16,632	522	152,792

used performance indexes, including sensitivity, specificity, precision, NPV, as well as F1 score, are also calculated and shown in Table XI.

3) Results of Sleep Quality Assessment: In this section, we evaluate the sleep quality of the two test subjects in home scenario. We recorded the four sleep quality parameters mentioned in Section III-C, including time in bed, number of times of bed leaving, number of times of body movements (i.e., turning over) all night, and standard deviation of the interval between body movements. We then use fuzzy inference to estimate the sleep quality of the two subjects throughout the night. In addition, we also superimposed the stress images of the subjects throughout the night so that we can understand the stress of various parts of the subject.

Fig. 21 shows the process of superimposing pressure images. The magnitude of the pressure images is first magnified by nine times, and all the pressure values are determined based on bilinear interpolation. After that, the pressure image is enlarged and smoothed with a Gaussian filter as that in

TABLE XI
PERFORMANCE INDICATORS OF THE PROPOSED CNN MODEL FOR THE RECOGNITION OF THE FOUR SLEEP POSTURES AT HOME TEST ENVIRONMENT

Performance Index \ Posture	Face Up	Face Right	Face Left	Face Down
Sensitivity	96.54%	97.26%	98.33%	100.00%
Specificity	97.60%	98.77%	98.83%	99.92%
Precision	98.04%	97.54%	91.13%	80.31%
NPV	95.77%	98.63%	99.79%	100.00%
F1 Score	97.29%	97.40%	94.59%	89.08%
Accuracy	96.99%			

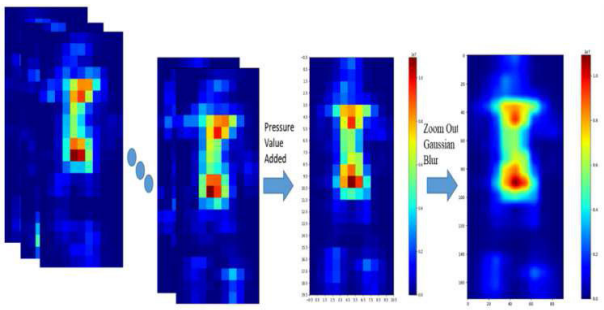

Fig. 21. Process of pressure images superposition for lying postures all night.

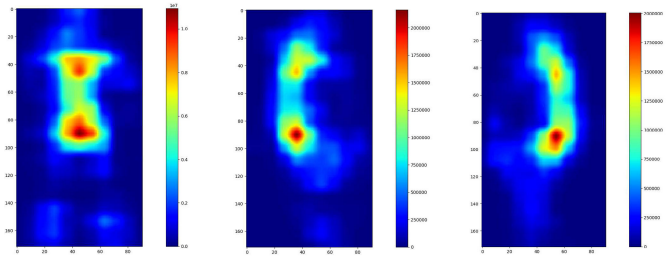

(a) (b) (c)

Fig. 22. Superimposed image results corresponding to the same sleep posture during the first night in home test scenario by subject No. 1. (a) Face up. (b) Face left. (c) Face right.

Section II-B.2. Finally, the enlarged and smoothed pressure images of the same posture are superimposed, which forms the rightmost image in Fig. 21. Fig. 22 shows the superimposed image results corresponding to different postures (including face up, face left, and face right) of subject number 1 all night. It can be seen that when lying face up, the pressure on the buttock and the back is obviously larger than other parts; when lying on the side, the buttock and the shoulder receive greater pressure.

We then further investigate the sleep quality of the two subjects on three nights. Based on the four sleep quality parameters recorded and the fuzzy inference rules mentioned in Section III-C, the subjects' sleep quality scores can be obtained. In this article, the center-of-gravity method is applied for the defuzzification process and shown in Fig. 23. With the fuzzy inference and defuzzification process, the score of sleep quality for subject No. 1 on the first night is 52.85 and that of subject No. 2 is 27.99.

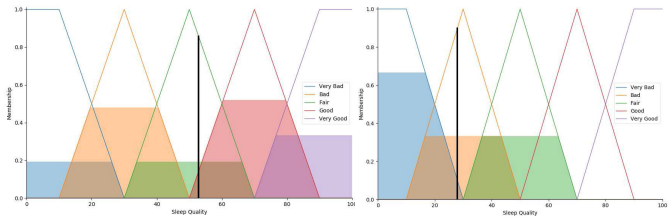

(a) (b)

Fig. 23. Defuzzification result of the two subjects at the first night (home scenario). (a) Subject No. 1. (b) Subject No. 2.

TABLE XII
TWO SUBJECTS' SLEEP QUALITY PARAMETERS AND EVALUATION FOR SIX NIGHTS

Subject ID	In Bed Time H: Min:Sec	Numbers of Times of Bed-Leaving	Numbers of Times of Body Movements all night	Standard deviation of Body Movements Time Interval	Sleep Quality Score	Sleep Quality
1	7:18:51	3	23	15.79	52.85	Fair
1	6:49:05	0	24	13.21	70.82	Good
1	7:09:09	1	26	12.91	74.90	Good
2	6:52:00	3	8	41.33	27.99	Bad
2	7:53:25	2	11	36.59	37.43	Bad
2	6:18:50	3	10	28.92	28.53	Bad

Table XII shows the detailed sleep quality parameters and the evaluation results of the two subjects for six nights. Subject No. 1 has good sleep quality on the other two nights except the first night's medium sleep quality. In general, subject No. 2 scores low in sleep quality, whose result of sleep quality rating is bad.

4) Comparisons With Prior Arts: In this section, the proposed pressure-sensor-based sleep status and quality evaluation system is compared with prior arts. A qualitative comparison in terms of functionalities provided by individual algorithm is given in Table XIII. Literature [25] also applied the use of pressure-sensing elements; however, work [25] cannot differentiate sitting and lying postures, which may be subject to a misinterpretation of results, nor can it provide sleep quality indicators. In [26], a 3×8 pressure-sensing array is proposed for sleep status detection. Although literature [26] defines some sleep quality indicators, it did not propose how to evaluate sleep quality. In addition, work [26] does not have the function of distinguishing between sitting and lying postures, and it also cannot identify various lying postures, so misclassification of the subject's status is prone to occur. Literature [29] uses a pressure-sensing mattress as well, the same as the foregoing literature in [25] and [26], and work [29] is subject to a misinterpretation of results due to the inability to differentiate sitting postures nor can it produce a method for determining sleep quality ratings. Works [35] and [36] use frequency-modulated continuous-wave (FMCW) and UWB wireless technology, respectively, and can accurately detect the user's sleeping posture and turning movements, allowing users to be monitored or protected in a more natural environment; however, works [35] and [36] do not provide sitting and lying posture recognition nor do they provide a sleep quality assessment mechanism.

In order that the readers can easily download all the materials required and reproduce the experimental results of the

TABLE XIII
QUALITATIVE PERFORMANCE COMPARISON WITH PRIOR ARTS

Functionality \ Prior Arts	Xu et al. [25]	Pino et al. [26]	Verhaert et al. [29]	Yue, et al. [35]	Piriyajitakonkij et al. [36]	Proposed
Sensing Element / Device	Pressure Sensor	Pressure Sensor	Pressure Sensor	FMCW	UWB	Pressure Sensor
Sitting and Lying Posture Differentiation	x	x	x	x	x	✓
Sleep Posture Recognition	✓	x	✓	✓	✓	✓
Turning Over Detection	✓	✓	✓	✓	✓	✓
Sleep Quality Inference	x	x	x	x	x	✓

proposed system, the source code, collected data, as well as the pretrained SVM and CNN models are all placed in GitHub. The URL of the uploaded materials of this article can be found in [39].

5) Limitations of the Proposed Approach: The proposed pressure-sensitive mattress can provide the subject with sleep status parameters (including time in bed, number of times of bed leaving, number of times of body movements (or turning over) all night, and standard deviation of the interval between body movements) and can also perform the primary sleep quality assessment. However, since the proposed system does not have the function of detecting important physiological parameters of the subject, it cannot replace the PSG examination yet. At this stage, the various parameters regarding sleep status (especially those related to human motion behavior) provided by the proposed system can complement the clinical deficiencies and serve as an aid to clinical diagnosis.

Besides the functionality constraints, since sudden death of newborn infants due to sleep asphyxia has been reported from time to time, we adopt a higher resolution pressure-sensing element placement strategy at the beginning of the system design in order to know the posture of newborn infants on the mattress and whether they had body movements so that we can send an alert message to parents in time. However, since the lying data of newborn babies are not easily available, the training data and test data used in this article are all adults; if this pressure-sensitive pad is extended to detect the posture of newborn babies in the future, the training data and verification data have to be collected separately.

V. CONCLUSION

This article proposes the use of pressure-sensing mattress system for long-term sleep status and quality monitoring. The readings of each node of the pressure-sensing mattress can be used to analyze or obtain the sleep parameters of the test subject's time in bed, number of times of bed leaving, number of times of body movements all night, standard deviation of body movements time interval, and the pressure distribution in each sleep posture all night; combined with the proposed fuzzy rules, it is possible to further evaluate the subjects' sleep quality all night. Differing from part of the prior arts which used wearable devices, the proposed system does not require the subjects to wear any devices, which avoids the subjects' discomfort and makes the subjects perform sleep quality analysis and test in the most natural scenario. In addition, the proposed system not only provides the aforementioned parameters related to sleep quality but also differentiates the subject's sitting and lying postures to extract the real time in bed. With the sleep posture recognition model, we can learn about the distribution of sleep postures and muscle pressure all night. In the future, if the proposed system can be combined with other devices with physiological parameters (such as heart rate, respiration rate, blood oxygen, blood pressure, and other important physiological parameters) or with PSG examination, it is believed that it will help to improve the effectiveness of sleep quality disorder analysis and contribute to clinical diagnosis.

REFERENCES

[1] I. Capellini, P. McNamara, B. T. Preston, C. L. Nunn, and R. A. Barton, "Does sleep play a role in memory consolidation? A comparative test," *PLoS ONE*, vol. 4, no. 2, p. e4609, Feb. 2009.

[2] (Apr. 14, 2015). *National Sleep Foundation. How Much Sleep Do We Really Need? Last Access*. [Online]. Available: http://www.sleepfoundation.org/article/how-sleep-works/how-much-sleep-do-we-really-need/

[3] *World Sleep Society, News, World Sleep Day*. Accessed: May 2020. [Online]. Available: http://worldsleepsociety.org/world-sleep-day

[4] J. Berglund, "The danger of sleep deprivation," *IEEE Pulse*, vol. 10, no. 4, pp. 21–24, Jul. 2019.

[5] *Sleep and Sleep Disorders*. Accessed: May 2020. [Online]. Available: http://www.cdc.gov/sleep/index.html

[6] J. S. Higgins, J. Michael, R. Austin, T. Akerstedt, and P. Hans, "Asleep at the wheel—The road to addressing drowsy driving," *Sleep*, vol. 40, no. 2, pp. 1–9, 2017.

[7] M. Hafner, M. Stepanek, J. Taylor, W. M. Troxel, and C. van Stolk, "Why sleep matters—The economic costs of insufficient sleep a cross-country comparative anslysis," *RAND Health Quart.*, vol. 6, no. 4, p. 11, 2017.

[8] (2019). *Annual Report of Taiwan Society of Sleep Medicine, Survey on Prevalence Rate of Chronic Insomnia and Sleep Problems Among Shift Workers*. [Online]. Available: http://www.tssm.org.tw/file/1563864454.pdf

[9] T. Young, P. E. Peppard, and D. J. Gottlieb, "Epidemiology of obstructive sleep apnea a population health perspective," *Amer. J. Respiratory Crit. Care Med.*, vol. 165, no. 9, pp. 1217–1239, 2002.

[10] C.-S. Huang, C.-L. Lin, L.-W. Ko, S.-Y. Liu, T.-P. Su, and C.-T. Lin, "Knowledge-based identification of sleep stages based on two forehead electroencephalogram channels," *Frontiers Neurosci.*, vol. 8, p. 263, Sep. 2014.

[11] C. Varon, A. Caicedo, D. Testelmans, B. Buyse, and S. Van Huffel, "A novel algorithm for the automatic detection of sleep apnea from single-lead ECG," *IEEE Trans. Biomed. Eng.*, vol. 62, no. 9, pp. 2269–2278, Sep. 2015.

[12] C.-E. Kuo, Y.-C. Liu, D.-W. Chang, C.-P. Young, F.-Z. Shaw, and S.-F. Liang, "Development and evaluation of a wearable device for sleep quality assessment," *IEEE Trans. Biomed. Eng.*, vol. 64, no. 7, pp. 1547–1557, Jul. 2017.

[13] C. Karmakar, A. Khandoker, T. Penzel, C. Schöbel, and M. Palaniswami, "Detection of respiratory arousals using photoplethysmography (PPG) signal in sleep apnea patients," *IEEE J. Biomed. Health Informat.*, vol. 18, no. 3, pp. 1065–1073, May 2014.

[14] H.-W. Tseng, C.-D. Huang, L.-Y. Yen, T.-W. Lin, Y.-W. Lee, and Y.-L. Chen, "A method of measuring sleep quality by using PPG," in *Proc. IEEE Int. Conf. Consum. Electron.-Taiwan (ICCE-TW)*, May 2016, pp. 1–2.

[15] P. Fonseca et al., "Validation of photoplethysmography-based sleep staging compared with polysomnography in healthy middle-aged adults," *Sleep*, vol. 40, no. 7, pp. 1–10, 2017.

[16] H. Yoon, S. H. Hwang, J.-W. Choi, Y. J. Lee, D.-U. Jeong, and K. S. Park, "Slow-wave sleep estimation for healthy subjects and OSA patients using R–R intervals," *IEEE J. Biomed. Health Informat.*, vol. 22, no. 1, pp. 119–128, Jan. 2018.

[17] C.-T. Lin et al., "IoT-based wireless polysomnography intelligent system for sleep monitoring," *IEEE Access*, vol. 6, pp. 405–414, 2018.

[18] A. Supratak, H. Dong, C. Wu, and Y. Guo, "DeepSleepNet: A model for automatic sleep stage scoring based on raw single-channel EEG," *IEEE Trans. Neural Syst. Rehabil. Eng.*, vol. 25, no. 11, pp. 1998–2008, Nov. 2017.

[19] H. Phan et al., "Towards more accurate automatic sleep staging via deep transfer learning," *IEEE Trans. Biomed. Eng.*, vol. 68, no. 6, pp. 1787–1798, Jun. 2021.
[20] A. Koushik, J. Amores, and P. Maes, "Real-time smartphone-based sleep staging using 1-channel EEG," in *Proc. IEEE 16th Int. Conf. Wearable Implant. Body Sensor Netw.*, May 2019, pp. 1–4.
[21] S.-Y. Chang et al., "An ultra-low-power dual-mode automatic sleep staging processor using neural-network-based decision tree," *IEEE Trans. Circuits Syst. I, Reg. Papers*, vol. 66, no. 9, pp. 3504–3516, Sep. 2019.
[22] X. Ran, C. Wang, Y. Xiao, X. Gao, Z. Zhu, and B. Chen, "A portable sitting posture monitoring system based on a pressure sensor array and machine learning," *Sens. Actuators A, Phys.*, vol. 331, Nov. 2021, Art. no. 112900.
[23] L. Samy, M.-C. Huang, J. J. Liu, W. Xu, and M. Sarrafzadeh, "Unobtrusive sleep stage identification using a pressure-sensitive bed sheet," *IEEE Sensors J.*, vol. 14, no. 7, pp. 2092–2101, Jul. 2014.
[24] D. Waltisberg, O. Amft, D. P. Brunner, and G. Troster, "Detecting disordered breathing and limb movement using in-bed force sensors," *IEEE J. Biomed. Health Informat.*, vol. 21, no. 4, pp. 930–938, Jul. 2017.
[25] X. Xu, F. Lin, A. Wang, Y. Hu, M.-C. Huang, and W. Xu, "Body-Earth Mover's distance: A matching-based approach for sleep posture recognition," *IEEE Trans. Biomed. Circuits Syst.*, vol. 10, no. 5, pp. 1023–1035, Oct. 2016.
[26] E. J. Pino, A. D. D. La Paz, and P. Aqueveque, "Noninvasive monitoring device to evaluate sleep quality at mining facilities," *IEEE Trans. Ind. Appl.*, vol. 51, no. 1, pp. 101–108, Jan. 2015.
[27] E. J. Pino, A. A. Moran, A. D. D. La Paz, and P. Aqueveque, "Validation of non-invasive monitoring device to evaluate sleep quality," in *Proc. 37th Annu. Int. Conf. IEEE Eng. Med. Biol. Soc. (EMBC)*, Aug. 2015, pp. 7974–7977.
[28] J. M. Kortelainen, M. O. Mendez, A. M. Bianchi, M. Matteucci, and S. Cerutti, "Sleep staging based on signals acquired through bed sensor," *IEEE Trans. Inf. Technol. Biomed.*, vol. 14, no. 3, pp. 776–785, May 2010.
[29] V. Verhaert et al., "Unobtrusive assessment of motor patterns during sleep based on mattress indentation measurements," *IEEE Trans. Inf. Technol. Biomed.*, vol. 15, no. 5, pp. 787–794, Sep. 2011.
[30] J. Ye, Y. Lin, Z. Li, J. Lee, A.-A. Abdulrahman, and M. Jin, "A non-invasive sleep analysis approach based on a fuzzy inference system and a finite state machine," *IEEE Access*, vol. 7, pp. 2664–2676, 2019.
[31] F. Deng et al., "Design and implementation of a noncontact sleep monitoring system using infrared cameras and motion sensor," *IEEE Trans. Instrum. Meas.*, vol. 67, no. 7, pp. 1555–1563, Jul. 2018.
[32] S. Akbarian, G. Delfi, K. Zhu, A. Yadollahi, and B. Taati, "Automated non-contact detection of head and body positions during sleep," *IEEE Access*, vol. 7, pp. 72826–72834, 2019.
[33] M. Gall et al., "Automated detection of movements during sleep using a 3D time-of-flight camera: Design and experimental evaluation," *IEEE Access*, vol. 8, pp. 109144–109155, 2020.
[34] W. Gu, L. Shangguan, Z. Yang, and Y. Liu, "Sleep hunter: Towards fine grained sleep stage tracking with smartphones," *IEEE Trans. Mobile Comput.*, vol. 15, no. 6, pp. 1514–1527, Jun. 2016.
[35] S. Yue, Y. Yang, H. Wang, H. Rahul, and D. Katabi, "BodyCompass: Monitoring sleep posture with wireless signals," *ACM Interact. Mob. Wearable Ubiquitous Technol.*, vol. 4, no. 2, pp. 1–25, Jun. 2020.
[36] M. Piriyajitakonkij et al., "SleepPoseNet: Multi-view learning for sleep postural transition recognition using UWB," *IEEE J. Biomed. Health Informat.*, vol. 25, no. 4, pp. 1305–1314, Apr. 2021.
[37] UNEO. (May 2015). *Specification for GD25-100N Rev 1.0*. [Online]. Available: https://www.uneotech.com/uploads/product_download/tw/GD25-100N%20ENG.pdf
[38] S. Ostadabbas, R. Yousefi, M. Nourani, M. Faezipour, L. Tamil, and M. Q. Pompeo, "A resource-efficient planning for pressure ulcer prevention," *IEEE Trans. Inf. Technol. Biomed.*, vol. 16, no. 6, pp. 1265–1273, Nov. 2012.
[39] (Feb. 2023). *Source Code, Collected Data, Pre-Trained Models, and Materials of the Paper*. [Online]. Available: https://github.com/JonesChau/Sleep-Parameter

Lih-Jen Kau (Senior Member, IEEE) was born in Hualien, Taiwan, in 1969. He received the B.S. degree in control engineering and the M.S. and Ph.D. degree in electrical and control engineering from National Chiao Tung University (NCTU), Hsinchu, Taiwan, in 1991, 1997, and 2008, respectively.

From 1996 to 1998, he was with Chunghwa Telecom, Taipei, Taiwan, where he served as a Senior Technician. In August 1998, he joined the Department of Computer and Communication Engineering, Dahan Institute of Technology, Hualien, as an Instructor, where he has been an Assistant Professor since February 2006. Since August 2009, he has been with the Department of Electronic Engineering (EE), National Taipei University of Technology (NTUT), Taipei. He is currently an Associate Professor with the Department of Electronic Engineering, NTUT. His research interests include image/video coding and processing, healthcare and biomedical information technology, and autonomous vehicle system integration.

Dr. Kau received the 2003 ZyXEL Scholarship Award from ZyXEL Communications Corporation, Hsinchu. He was a recipient of the Best Live Demonstration Award at the 2016 IEEE Biomedical Circuits and Systems Conference and the Best Paper Award at the 2019 IEEE International Conference of Intelligent Applied Systems on Engineering.

Mao-Yin Wang was born in Tainan, Taiwan, in 1979. He received the B.S. degree in electronic engineering from the Lan Yang Institute of Technology, Yilan, Taiwan, in 2003, and the M.S. degree in computer science from National Chengchi University (NCCU), Taipei, Taiwan, in 2012. He is currently pursuing the Ph.D. degree in electronic engineering with the National Taipei University of Technology (NTUT), Taipei.

From 2003 to 2005, he was with VisionBank Technology Corporation, Hsinchu, Taiwan, as a Field Application Engineer. From 2005 to 2008, he was with ALLTEK Technology Corporation, Taipei, as a Field Application Engineer. From 2008 to 2015, he was with YUBAN & Company, Taipei, as a Product Manager. Since March 2015, he has been with Silicon Application Corporation, Taipei, as a Product Manager. His research interests include biomedical information processing, motor control system design, and automotive driver circuit design for traction inverters.

Houcheng Zhou was born in Guangdong, China, 1991. He received the B.S. and M.S. degrees in electronic engineering from the National Taipei University of Technology (NTUT), Taipei, Taiwan, in 2016 and 2020, respectively.

From December 2020 to April 2022, he worked with China BYD Automobile Industry Company Ltd., Shenzhen, China, as an Electronic Engineer. He is currently a Data Analyst at the Shenzhen Health Development Research and Data Management Center, Shenzhen, Guangdong, China. His research interests include biomedical signal processing and image processing.